Measurement of the Interaction Force among Particles in Three-Dimensional Plasma Clusters

T. Antonova, B. M. Annaratone, D. D. Goldbeck, V. Yaroshenko, H. M. Thomas, and G. E. Morfill

Max-Planck Institut für extraterrestrische Physik, D-85740 Garching, Germany

(Received 3 March 2005; published 20 March 2006)

The interaction forces between particles have been studied in a 3D plasma cluster under weak external confinement. A suitable combination of dc and rf applied to a small electrode provided gravity compensation, uniform over dimensions much larger than the cluster itself. The forces acting on the particles could be reconstructed due to unique three-dimensional diagnostics, which allow us to obtain coordinates and velocities of all the particles simultaneously. The measurements yield a maximum (external) confinement force of $1.4 \times 10^{-15} N$ and interparticle force that is repulsive at short distances and attractive at larger distances, with a maximum attractive force of $2.4 \times 10^{-14} N$ at particle separation 195 μm.

DOI: 10.1103/PhysRevLett.96.115001 PACS numbers: 52.27.Lw

Ionized gas containing charged particles (complex plasmas) is a subject of considerable interest in fundamental physics, plasma science, and astrophysics, as well as technological applications. These include strong coupling phenomena, limits of cooperative behavior, viscoelastic properties, phase transition, critical point phenomena, etc., as well as interstellar clouds, planet formation (planetary rings, comet tails) and dust in fusion reactor, self-assembly of materials, plasma medicine, etc. [1–4].

On Earth, the balance between gravity and electric field usually confines the particle clouds near the lower plasma boundary, leading to flat (essentially two-dimensional) crystallized or fluid assemblies [5]. Under microgravity the particles assemble in structures with empty spaces (voids) and sharp boundaries. A fundamental issue is the nature and form of the (binary and collective) interaction forces between the microparticles, which give rise to the observed phenomena. There is a growing theoretical and experimental interest in the possibility of attraction between particles in a plasma [6–10], with experimental techniques using collisions [9] and laser manipulation [10]. In the present work repulsive or attractive forces among particles suspended in a plasma are estimated for the first time from the observation of their spontaneous motion in three-dimensional plasma clusters. The main features of these measurements are (1) weak (external) confinement, (2) that the particles levitate inside the plasma region and not in the plasma sheath, (3) that the particle number in the clusters can be externally controlled, (4) novel 3D diagnostics, which allows us to reconstruct the kinetic of the particles. The possibility to get 3D plasma clusters was already pointed out in the work of Arp *et al.* [11] using strong external confinement and ''scanned'' visualization. Our work is complementary to [11], since we use completely different systems to ''construct'' and characterize 3D plasma clusters.

Experimental setup.—The experiments have been performed in the so-called PKE-Nefedov chamber, which consists of two parallel plate electrodes and glass walls. The upper one is radiofrequency (rf) driven at 13.56 MHz, the lower electrode being grounded, apart from a small central ''pixel,'' 3.8×3.8 mm^2, which can be independently driven in dc and rf. Typical conditions are rf voltage on the upper electrode in the range of 200–300 V_{pp}, about 150 V_{pp} in ''push-pull'' on the lower central pixel, Argon pressure from 35 to 70 Pa and melamine-formaldehyde particles of 3.4 μm diameter. More details about the ''adaptive'' electrode are given in Ref. [12]. Initially, the particles injected in the plasma form the usual 2D cloud at the plasma-sheath edge, where the electric field is compensated by gravity. Then, by suitably adjusting dc and rf on the central pixel, a glow region is formed above the electrode, that is much brighter than the bulk plasma. Here particle clusters can be assembled [13]. The particle number in the cluster can be controlled by varying the rf applied to the pixel. We investigated 3D clusters from 4 up to 73 particles, with cluster diameters ranging from 0.35 mm up to 0.9 mm. Since the microparticles all carry negative charges, one would presume that internal electrostatic pressure would disperse the cluster without strong additional confinement. External confinement can, in principle, be due to electrostatic fields, ion or neutral drag or pressure. In addition, there could be attractive force between the charged particles.

Three-dimensional diagnostics.—To get all three position and velocity coordinates simultaneously for each particle is a challenge in experimental complex plasma science. With our diagnostic setup we can get all particle coordinates as a function of time. The particle distribution is illuminated by two parallel laser beams (686 and 656 nm) of complementary intensity and the scattered light is recorded at an optimal angle of 68° by two selective CCD-cameras. The particle image corresponds to instantaneous particle position in the xy direction, the z coordinate being given by the ratio of the two lasers' scattered light intensity. The simultaneity is absolutely indispensable to determine the dynamical behavior of the particles. The velocity vector was determined mainly by the 3D traces left by the particles during the CCD opening $t = 36$ ms. To improve the resolution in the z direction, positions and

TABLE I. Estimated values for the floating potential on isolated particles according to different theories. The charge on the particles, the electric field needed for levitation and the energy acquired by the ions in a m.f.p. are also shown.

Theory	O.M.L.	A.B.R.	A.B.R. (collis.)
$V_f(kT_e)/e$	2.1	0.33	0.533
charge (e)	24 814	3899	6298
$\vec{E}_{\text{levitation}}$ (V/m)	76.5	486.9	301.5
$\text{Energy}_{\text{ions, 1 m.f.p.}}$ (eV)	2.3×10^{-3}	1.5×10^{-2}	9.1×10^{-3}

velocities are determined also by an additional illumination from an infrared laser (785 nm), with the light collected by a third camera at 90° with respect to the other two cameras. The three cameras provide synchronized time sequences (25 frames/s, total viewing time 8 s). Static particles have an error in the position measurement of 3 μm in x and z directions and of 21 μm in the y direction.

Particle charge.—The charge on the particles can be estimated from different theories, see Table I.

The orbital motion limited (OML) [14] theory is not applicable in our range of pressures because typical values of the mean free path (m.f.p. = 30 μm at 60 Pa) are much shorter than the Debye length, which is about 100–160 μm using a plasma density of 10^{16}–10^{15} m^{-3}, deduced from the bright glow, and an electron temperature of 5 eV (somewhat higher than the main discharge). The Allen-Boyd-Reynolds theory for radial motion (ABR) [15] and the moderate collisional regime [16] are based on the hypothesis of "cold" ions. They could be applied here. The actual floating potential acquired by a particle in the cluster is reduced with respect to an isolated particle due to the presence of the nearby particles. We therefore believe that a reasonable estimate of the charges lies between 3000 to 5000e.

Description of particle kinematics.—We analyze here the dynamical behavior of a cluster consisting of 4 particles: A, A1, A2, D [Fig. 1(a)], interacting with a fifth (B) orbiting below the cluster. Particles orbiting in a plasma have often been observed in dc and rf experiments [17]. The cluster is periodically distorted by the motion of the lower particle. At some point, due to thermal vibrations, the distance between a cluster particle A and the orbiting particle B becomes shorter than the distance to the upper cluster particle D. In this case particle A breaks its bond with the upper particle D and starts to move in the direction of the orbiting particle B [Fig. 1(b)]. As soon as particle B proceeds further and the distance AB increases, particle A returns back and takes its place inside the structure, "pushing" on its neighbors to restore equilibrium. The motion of particle B is almost elliptical, this will be used later to estimate the external confinement force. The particle separation distance as a function of time for particles A, B and A, D is shown in Fig. 2, which allows us to determine the interparticle interaction force in this distance range. We note here that for separation >0.3 mm the particles do not interact, while the maximum force occurs at about 0.2 mm.

Analysis of forces in small clusters.—The force has been derived from the kinematics of the motion $\sum_i \vec{F}_i = M\ddot{\vec{x}} + \gamma\dot{\vec{x}}$, where M is the mass of the particle and γ is the neutral drag constant given for spheres by Epstein [18]. In our calculations we used the coefficient for diffuse reflection with accommodation ($\delta = 1.442$). At the Argon pressure for our experiment the inertia is always much smaller than the neutral drag. From the 3D trace left by a moving particle we derived the vector velocity, from which we determined the instantaneous vector force acting on a particle. This force is due to systemic forces as well as the influence of all the other particles' fields.

In order to separate these components we proceed in the following way: (1) by assuming that the orbital motion of particle B is due to external confinement field only, we may estimate the maximum strength of this force, and (2) by assuming that the main contribution to the force on particle A is due only to the nearest two neighbors, we

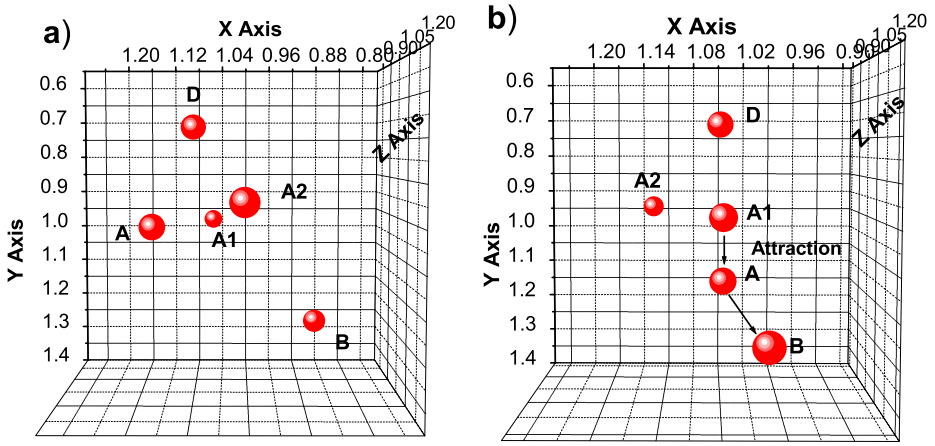

FIG. 1 (color online). A cluster of 4 particles. (a) Particles before interaction, (b) particle A is attracted by the orbital particle B. Units on the axis are in millimeters. ($P = 57$ Pa, peak-to-peak voltage are $V_{\text{rf pixel}} = 120$ V, $V_{\text{rf driven electrode}} = 300$ V). Depth visualization uses variation in particle (sphere) size, larger spheres are "closer" (have higher z values) than smaller spheres.

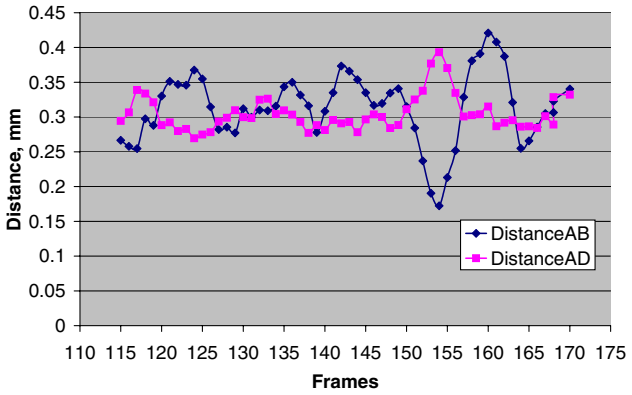

FIG. 2 (color online). Distance between particles A and B, and A and D. The two peaks at frame 155 correspond to attraction.

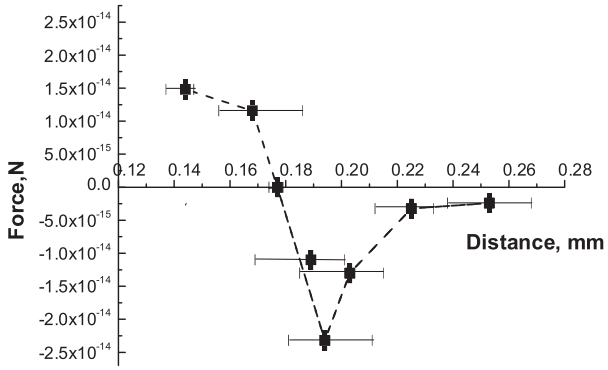

FIG. 3. Measured force among particles with respect to distance.

can estimate the pair-interaction force from the kinematics of the motion. In the first approximation we derive the upper limit for an external confinement force by equating it with the measured centripetal force, which acts on the rotating particle. Using a mean orbit radius of 0.219 mm the maximum estimated centripetal force $F = MV^2/r$ is $1.4 \times 10^{-15}N$ at the maximum velocity of 3.2 mm/sec and the minimum force is $0.55 \times 10^{-15}N$ at the minimum velocity of 1.97 mm/sec. A more detailed orbit investigation did not show any particular radius dependence. Also, this particle is only 387 μm above the electrode, which implies that its vertical deflection due to other forces is correspondingly small.

From the second component of the force due to nearby particles we can derive the pair-interaction force solving the following equations:

$$F(d1)\cos\alpha + F(d2)\cos\beta = \gamma V, \quad (1)$$

$$F(d1)\sin\alpha + F(d2)\sin\beta = 0, \quad (2)$$

where $F(d1)$ and $F(d2)$ are the forces as functions of distances with respect to the two nearest particles in each frame, α and β are the angles between the line connecting the particles and the trajectory, and V is the relative velocity.

The sign of the forces $F(d)$ is estimated using both the previous and the successive frame. The result is shown in Fig. 3. One can see that the maximum attractive force (negative part of the plot) occurs at the interparticle distance 0.194 mm and it is fairly high, $2.4 \times 10^{-14}N$. For separation larger than 0.25 mm the attractive force rapidly goes to zero and the particles essentially do not interact any more. If the distance between particles is less than 0.177 mm, they repel each other. The error bars are due to the pixel discretization of particle position and trace. (Note that changing the value for δ will lead to a rescaling of the vertical axis, but will not alter the generic shape of the curve). From these measurements it is clearly seen that the centripetal force (and by implication an external confinement force) is much smaller than the measured interactive force among particles in this cluster. Hence, the particle motion cannot be explained using external confinement alone.

Attractive forces in medium size clusters.—Here we analyze a cluster of 73 particles, where both systemic and collective attractive force may exist. In the recorded time sequence one of the particles is very mobile (Fig. 4). This particle has an orbital trajectory with the radius $r =$ 0.275 mm, which most of the time is external to the cluster. The full orbit takes about 0.4 sec, the maximum velocity is 1.26 mm/sec. During this external motion the average distance from the nearest particle in the cluster is 0.181 mm, the minimum distance is 0.162 mm, and the maximum distance 0.198 mm. Since the particle may escape from the cluster but cannot leave it completely, there must be an attraction force which balances the centripetal force. From the particle dynamics, observed radius of curvature ($r = 2.84$ mm), etc., this force is calculated to be $1.7 \times 10^{-16}N$. It may not be the highest value, because the radius is determined by a balance of the attractive force and by the repulsion from the outer shell of the cluster. We

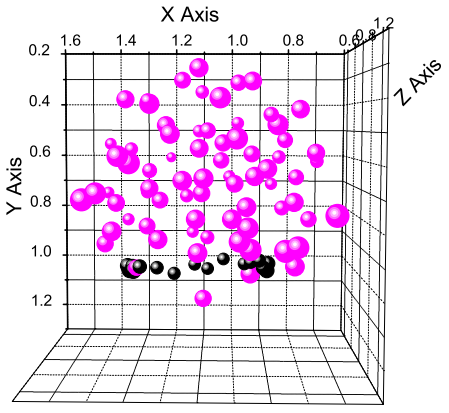

FIG. 4 (color online). Cluster of 73 particles. The black spheres show the positions of the moving particle in 15 consecutive frames (0.6 sec), gray (pink) spheres—the position of other particles in cluster, which are almost stable in time. Units on the axis are in millimeters.

do not have a direct measurement of the confinement in this case.

Discussion.—Our experiments have provided new information regarding the binary and collective interaction processes in complex plasmas. In a weakly confined system, particle clusters of various size were assembled and the individual particle dynamics was studied.

For small clusters we may assume that collective effects are not important and that the particle dynamics is dominated by binary interactions and the external confining field. The force due to the later was calculated from the particle orbit ($\sim 10^{-15} N$). The binary interaction was calculated by assuming (in a small 4 particle cluster) that nearest neighbor effects dominate. This yielded a repulsive force at small particle separation (<0.17 mm)—as expected from electrostatic interaction—and an attractive force at larger distances, with a maximum attractive force of $2.4 \times 10^{-14} N$ (see Fig. 3). Since this force is more than an order of magnitude larger than the calculated (systemic) confining force, we believe that we have been able to identify (for the first time) an attractive component of the binary interaction between particles in plasma, not in the sheath. There are different theories about such interaction: (1) the vertical ''pairing'' observed in plasma sheath [10] caused by wake effects in the presheath streaming ions. This situation does not apply to our experiment, which was conducted in plasma; we accordingly did not observe any particle alignment. However, in the presence of strong ionization we cannot rule out particle interaction related to the ion drifting in the presheath; (2) there could be an attractive force due to induced dipoles caused by charge redistribution in the field of the nearest neighbor particle. This process is believed to be important in ''supercoagulation'' or gelation phase transition [19]. The force due to such an induced dipole would vary as r^{-4}, which is compatible with our measurements (Fig. 3); (3) attraction can also be produced by the so-called ''shadow force''—the mutual shielding of plasma (or neutrals) providing an attractive pressurelike force that varies as r^{-2}. Within the experimental uncertainties this may also just be feasible (Fig. 3).

In large clusters (investigated in a separate experiment) collective effects should dominate (e.g., double-layer formation at the surface of the cluster [4]) and binary interaction processes may be expected to be masked by these. The attractive force in the large (73 particle) cluster was measured at a mean distance from the central axis of 0.275 mm, that is much larger than a distance of 0.16 mm in the small (4 particle) cluster, which was used to measure the confinement. Therefore, the confinement measured for a small cluster cannot be taken as a confinement for a large one.

Since in the small cluster we may safely assume that the external (systemic) confinement is not modified by the microparticles, we believe that the $\sim 10^{-15} N$ force measured is due to the field produced by the shaped plasma from the pixel electrode. The large cluster, because of the larger dimensions ($r = 0.45$ mm), however, modifies the ion and electron population by recombination and by the changes in effective plasma potential, reducing the confinement. We suggest here that the effects of collective forces may have been seen for the first time. In a future series of experiments we will investigate this possibility systematically.

Conclusion.—In this Letter we have presented direct measurement of the presence of strongly localized attractive forces between like-charged microparticles in a small plasma cluster, and have found the indication of the existence of collective forces in larger particle assemblies.

We would like to thank Herr Steffes for the continuous assistance. This research was founded by Das Bundesministerium für Bildung und Forschung durch das Zentrum für Luft- und Raumfahrt e.V. (DLR) unter dem Förderkennzeichen 50 RT 0207.

[1] A. Bouchoule, *Dusty Plasmas: Physics, Chemistry and Technical Impacts in Plasma Processing*, edited by A. Bouchoule (Wiley, New York, 1999).
[2] P. K. Shukla and A. A. Mamun, *Introduction to Dusty Plasma Physics* (Institute of Physics Publishing Ltd., Bristol, 2002).
[3] S. V. Vladimirov and K. Ostrikov, Phys. Rep. **393**, 175 (2004).
[4] V. E. Fortov, A. G. Khrapak, S. A. Khrapak, V. I. Molotkov, and O. F. Petrov, Phys. Usp. **47**, 447 (2004).
[5] H. Thomas, G. E. Morfill, V. Demmel, J. Goree, B. Feuerbacher, and D. Mohlmann, Phys. Rev. Lett. **73**, 652 (1994).
[6] B. M. Annaratone, J. de Physique IV **7**, C4 (1997).
[7] A. M. Ignatov, Plasma Phys. Rep. **22**, No. 7, 585 (1996).
[8] S. A. Khrapak, A. V. Ivlev, and G. Morfill, Phys. Rev. E **64**, 046403 (2001).
[9] U. Konopka, G. E. Morfill, and L. Ratke, Phys. Rev. Lett. **84**, 891 (2000).
[10] A. Melzer, V. A. Schweigert, and A. Piel, Phys. Rev. Lett. **83**, 3194 (1999).
[11] O. Arp, D. Block, A. Piel, and A. Melzer, Phys. Rev. Lett. **93**, 165004 (2004).
[12] B. M. Annaratone, M. Glier, T. Stuffler, H. Thomas, M. Raif, and G. E. Morfill, New J. Phys. **5**, 92 (2003).
[13] B. M. Annaratone, T. Antonova, D. D. Goldbeck, H. M. Thomas, and G. E. Morfill, Plasma Phys. Controlled Fusion **46**, B495 (2004).
[14] J. E. Allen, Phys. Scr. **45**, 497 (1992).
[15] C. M. C. Nairn, B. M. Annaratone, and J. E. Allen, Plasma Sources Sci. Technol. **7**, 478 (1998).
[16] Paul Bryant, J. Phys. D: Appl. Phys. **36**, 2859 (2003).
[17] B. M. Annaratone and G. E. Morfill, J. Phys. D: Appl. Phys. **36**, 2853 (2003).
[18] P. S. Epstein, Phys. Rev. **23**, 710 (1924).
[19] A. V. Ivlev, G. E. Morfill, and U. Konopka, Phys. Rev. Lett. **89**, 195502 (2002).
[20] B. M. Annaratone *et al.*, Phys. Rev. E **66**, 056411 (2002).